

VANADIUM OXIDE NANOSTRUCTURES FOR LITHIUM BATTERY APPLICATIONS

Lin Xu¹, Liqiang Mai^{1,2,*}, Chunhua Han¹, Xu Xu¹, Yanzhu Luo¹

1. State Key Laboratory of Advanced Technology for Materials Synthesis and Processing, Wuhan University of Technology, Wuhan, 430070, China

2. Department of Chemistry and Chemical Biology, Harvard University, Cambridge, Massachusetts 02138, USA

*E-mail address: mlq@cmliris.harvard.edu

Introduction

Lithium and Lithium-ion batteries for portable electronic devices and hybrid electric vehicles have gained great importance for energy storage today. However, how to prepare cathode materials with higher energy density, high potentials, and longer cycle life is still a challenge. Compared with commercial LiCoO₂, vanadium oxides have higher specific capacity and interesting layered structures, which permit a wide variety of other molecules or cations to intercalate into the layers. This makes vanadium oxides such as V₂O₅, VO₂, V₆O₁₃, VO_x·H₂O, LiV₃O₈, vanadium oxide gels, NH₄V₄O₁₀, silver vanadium oxides, etc. likely to have the potential to offer much higher capacities. However, vanadium oxides are limited by fast capacity fading due to a decrease of the lithium diffusion coefficient D_{Li} and low electrical conductivity at the state of discharge. Recently, nanostructured cathodes are found to have excellent cycling performance because nanostructured materials have higher surface area, shorter Li ion diffusion lengths, and facile strain relaxation upon electrochemical cycling. Here we mainly review some typical nanostructured vanadium oxides such as VO_x nanotubes, VO₂ nanowires, V₂O₅ nanowires/nanorods, VO_x·H₂O nanowires, silver vanadium oxide nanowires, etc. and their applications in lithium batteries based on the recent research and our group's results.

VO_x nanotubes

Vanadium oxide (VO_x) nanotube is a kind of novel nanostructured vanadium oxides, which has potential applications in lithium batteries. The advantages of vanadium oxide nanotubes (VONTs) are large surface areas (including the inner surface and the outer surface), a short diffusion path in the nanotubes, which enable high electrochemical activity for lithium battery applications.^[1,2]

The main approach to prepare vanadium oxide nanotubes and some other nanotubes was with use of organic molecules as structure-directing agents. The interaction between organic molecules and inorganic precursors could be coordinative interactions, electrostatic interactions, or even hydrogen bonding. This method has opened a way to controlled synthesis for template-based periodic inorganic structures. Our group^[3] have prepared pure, Mo-doped, and Ag-

modified vanadium oxide nanotubes respectively via a rheological phase reaction followed by a self-assembling process, as shown in Fig.1. This as-obtained nanotubes material which is available in gram amounts is mostly constructed in a scroll-like fashion. The tube diameters can be tuned from a few nanometers to several hundreds of nanometers.

For the pure VONTs, the typical nanotube length is about 4 μm while the length could range from 1 to 10 μm. The diameter ranges from 30 to 100 nm. Lengths and diameters of the nanotubes depend on the conditions of the preparation, such as different template molecules, concentration and reaction time. The nanotube walls consist of 3-10 vanadium oxide layers. The distance between the vanadium oxide layers determined by electron diffraction is 2.88 nm.

For all of Mo-doped VONTs, it should be emphasized that when the doping is in the range of about 0–10 mol% the morphology and structure of the nanotubes are similar, and the differences concern inter-wall distances between oxide walls. In contrast with the undoped sample, the distance between the oxide layers increases from 2.88 to 2.93 nm of VONT with Mo doping content of 1 mol%.

Ag-modified VONTs have been prepared by adding Ag₂O to the V₂O₅ as the starting materials. In comparison with the pure VONTs, the Ag-containing nanotubes have shorter lengths (0.5-2 μm), a wider average outer diameter (70-110 nm) and a narrower inner diameter (10-30 nm). Interestingly, HRTEM images for the areas in the hollow tubes and between the VO_x layers of nanotube wall shows an obvious fringe with a regular spacing of ~0.23 nm, which is indexed to the inter-plane distance of (111) for Ag.

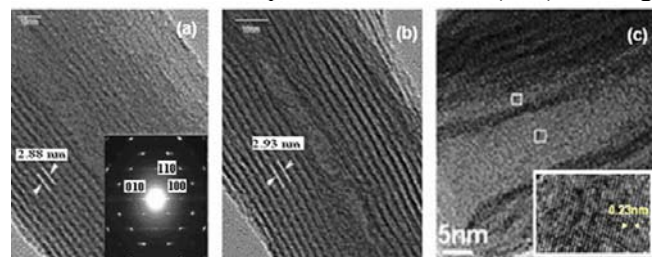


Fig.1: The HRTEM images of VONT (a), V_{0.99}Mo_{0.01}ONT (b), Ag-containing VONT (c).^[3]

The increase of interlayer distance between oxide layers in the (V_{0.99}Mo_{0.01})_xONTs results in more Li

sites and an improved electrochemical performance. Moreover, the electrochemical performance of $(V_{0.99}Mo_{0.01})_x$ ONTs is further enhanced by removing the residual organic template by heating in an inert atmosphere (Fig.2a). In Fig.2b, It is noted that the first discharge capacity of Ag-containing VONTs (234 mAh/g) is higher than that of the pure VONTs (185 mAh/g). Meanwhile, the former exhibits better cycling properties than the latter. Furthermore, the conductivity is at a magnitude of 10^{-7} S/cm for pure VONTs and 10^{-5} S/cm for Ag-VONT sample. Therefore, the improved electrical properties of Ag-VONTs results from higher conductivity.

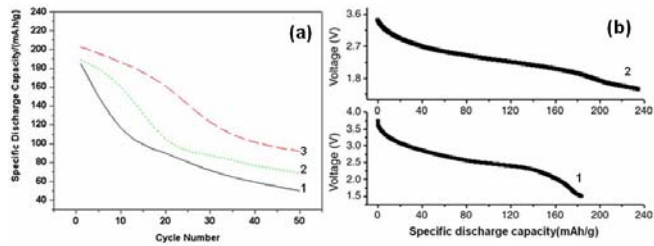


Fig.2: (a) The specific discharge capacity of VONT (1), $V_{0.99}Mo_{0.01}$ ONT (2) and heated $V_{0.99}Mo_{0.01}$ ONT (3), (b) first discharge cure of pure (1) and Ag-containing (2) VONTs.^[3]

VO₂ nanowires

Our group have synthesized VO₂ (B phase) nanowires^[4] via the rheological self-assembling method from V₂O₅ and CTAB. The sample consists of straight nanowires with uniform diameters in the range 40–60 nm, and lengths ranging from 1–2 mm. The aspect ratio of the corresponding nanowires lies in the range of 25–40. Lengths and diameters of the nanowires depend on the conditions of the preparation, such as different template molecules, concentration and reaction time.

The specific charge and discharge capacity for the VO₂ (B) nanowires grown by the rheological self-assembling process are 254 and 247 mAh/g, respectively^[4]. The cycling efficiency for the first 30 times exceeds 95.0% (Fig. 3). In contrast to normal VO₂ crystal material whose reversible capacity is approximately 160 mAh/g, VO₂ nanowires possess better electrochemical property.

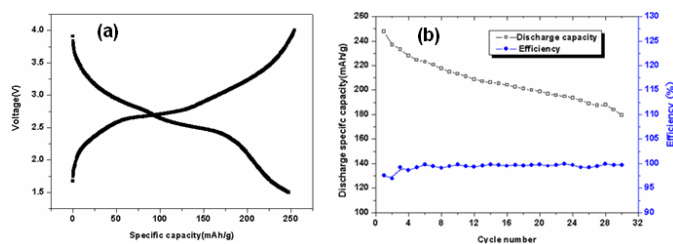


Fig.3: Initial charge/discharge curve of VO₂(B) nanorods(a), the curves of discharge specific capacity and efficiency vs. cycling number (b).^[4]

Recently, our group reported the stable surface functionalization and Langmuir-Blodgett (LB) assembly of VO₂ nanowires^[5]. VO₂ nanowires were functionalized with steric acid (SA) and CTAB, and then resuspended in chloroform. The chloroform VO₂ nanowire suspension was spread dropwise on the aqueous phase of a LB trough.

The XRD pattern of VO₂ nanowire LB films (Fig.4) only exhibits (00*l*) peaks, while diffraction peak characteristic of other crystalline planes are absent, showing that the VO₂ nanowires in LB film have a well-defined (00*l*) crystal plane orientation. To investigate the cause of orientation, we deposited LB film under low surface pressure and the same phenomenon occurred, suggesting that the observed orientation is not caused by pressure. Meanwhile, we also observed the well-defined (00*l*) plane orientation of the transferred films of VO₂ nanowires functionalized only by SA. We speculate that the VO₂ nanowires on water subphase reorient such that their (00*l*) crystal planes are parallel to the water/air interface, which results in the formation of oriented VO₂ nanowire Langmuir-Blodgett film. During the transfer process, this ordered structure remains. Although the mechanism for (00*l*) plane orientation of VO₂ nanowire LB films is still open, we believe that monodispersed functionalization and resulting uniform distribution provide the possibility for orientation of VO₂ nanowire LB film. Because the VO₂ nanowire surface has a large number of O-H bond and V-O bond groups, and the most closely packed (00*l*) crystal planes have the higher energy and more atoms, SA molecular and CTAB-SA complexes preferentially coordinate to the (001) surface thereby driving the orientation.

Electrochemistry of this VO₂ nanowire film has been investigated. The tenth cycle efficiency Q_{10} of VO₂ nanowire film before and after LB assembly is 98% and 99%, respectively, which shows huge enhancement in cycleability compared with V₂O₅ xerogel film mentioned in our previous study.^[6] Before LB assembly, the current density after enlarging 400 times has the same orders of magnitude to that after LB assembly, which shows that the current density and specific capacity of VO₂ nanowires LB films are approximately two orders higher than those of the VO₂ nanowire film before LB assembly, which is attributed to formation of VO₂ nanowire monolayers.

Moreover, in the cyclic voltammogram (CV) curves before and after LB assembly, only one oxidation peak was recorded corresponding to a two electron-transfer process, which is different with non-Nernstian redox couples and slow rate for the charge-transfer reaction of V₂O₅ films confirmed by the observation of two oxidation peaks. These differences can be explained by taking into account orientated and locally ordered structure of VO₂ LB film which is helpful to

insertion/extraction and transfer of Li ions and makes the process quicker and more reversible.

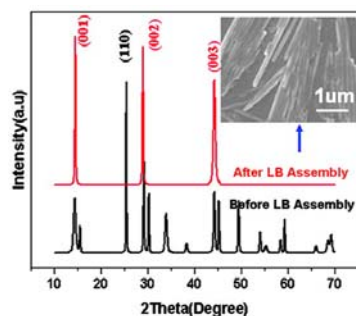


Fig.4: XRD patterns of VO_2 nanowires before and after LB assembly, insert is SEM image of VO_2 nanowire LB film.^[5]

V_2O_5 nanowires/ nanorods

Recently, nanostructured V_2O_5 such as nanowires, nanorods, nanotubes, and nanoribbons has been extensively studied to improve its electrochemical properties due to its short diffusion lengths for the lithium ions, a high contact surface area among the active materials, conductive additives and electrolyte, and good flexibility for volume changes during the electrochemical cycling.

During the discharge process, the structural transitions of crystalline V_2O_5 can be reflected in the discharge curve as three plateaus at 3.4, 3.2, and 2.3 V for the α / ϵ , ϵ / δ , δ / γ two-phase regions, respectively. ω - $\text{Li}_3\text{V}_2\text{O}_5$ forms at a deep discharge state. Chernova et al^[7] present the evolution of the cycling ability of V_2O_5 with morphology changing from micro- to nanocrystalline. The best capacity and cycling stability is demonstrated by the V_2O_5 nanorods synthesized by the annealing of $\text{H}_x\text{V}_4\text{O}_{10} \cdot n\text{H}_2\text{O}$ nanorods in oxygen. Ban et al^[8] found that when V_2O_5 nanorod-based lithium battery was cycled galvanostatically between 1.75 and 4.0 V, there was a slight overcharge on each cycle, which was associated with reaction with the electrolyte. This was solved by the addition of a small amount of lithium bis(oxalate)borate (LiBOB) to the electrolyte LiPF_6 , leading to a more effective protective layer.

Chou et al^[9] synthesized V_2O_5 nanoribbons by an ultrasonic assisted hydrothermal method and combined with a post-annealing process. Interestingly, the nanoribbons were composed of small nanoflakes. the nanoparticle has a porous structure on the surface with diameters less than 5 nm, which accounts for the high surface area. They reported that the possible reason for the formation of the pores is that the surfactant (Brij 30) could etch the surface of the raw V_2O_5 materials, and show a surface porous structure after annealing. Owing to high surface area, porous V_2O_5 nanoribbons show the best capacity of 430 mAh/g for initial discharge, the best cyclability (270 mAh/g for the 50th cycle), good high-rate capability (119 mAh/g at 2 C current density). The room temperature ionic liquid (RTIL)

electrolyte used in their work can prevent the dissolution of V_2O_5 during charge and discharge.

Chan et al^[10] synthesized V_2O_5 nanoribbons by a chemical vapor transport method, and studied lithium ion insertion in single V_2O_5 nanoribbons via chemical lithiation with n-BuLi. They found that transformation of α - V_2O_5 into the δ - $\text{Li}_3\text{V}_2\text{O}_5$ phase depends not only on the width but also the thickness of the nanoribbons. The transformation can take place within 10 s in thin nanoribbons, suggesting a Li diffusion constant 3 orders of magnitude faster than in bulk materials, resulting in a significant increase in battery power density (360 C). Meanwhile, efficient electronic transport can be maintained to charge a $\text{Li}_3\text{V}_2\text{O}_5$ nanoribbon within less than 5 s.

$\text{VO}_x \cdot \text{H}_2\text{O}$ nanowires

$\text{V}_3\text{O}_7 \cdot \text{H}_2\text{O}$ is one of the vanadium oxyhydroxides containing V^{5+} and V^{4+} in a ratio of 2 to 1, which is of interest because of the layered structure and redox activity. The layered structure of $\text{V}_3\text{O}_7 \cdot \text{H}_2\text{O}$ contains VO_6 octahedra and VO_5 trigonal bipyramids with vanadium oxidation states of +4 and +5, respectively. The water molecule is bound to the vanadium ion by replacing one of the oxygen atoms in the VO_6 octahedron and forms hydrogen bonds with the octahedral in the next layer. Qiao et al^[11] have synthesized $\text{V}_3\text{O}_7 \cdot \text{H}_2\text{O}$ nanowires via hydrothermal treatment of commercial V_2O_5 powder at relatively low temperatures. The synthetic process is free of any templates and reducing agents. The resulting $\text{V}_3\text{O}_7 \cdot \text{H}_2\text{O}$ nanowires are 100–500 nm in width, several tens to several hundreds micrometers in length, and about 20 nm in average thickness. The typical width-to-thickness ratios were about 5–20. They reported that the $\text{V}_3\text{O}_7 \cdot \text{H}_2\text{O}$ nanowires exhibited an initial high discharge specific capacity of 253.0 mAh/g in the potential range of 3.8–1.7 V and its stabilized capacity still remained 228.6 mAh/g after 50 cycles. All these results indicate that the $\text{V}_3\text{O}_7 \cdot \text{H}_2\text{O}$ nanowires are promising cathode materials in lithium-ion batteries.

$\text{VO}_x \cdot \text{H}_2\text{O}$ nanowires have been fabricated by rheological self-assembling process in our group. Here V_2O_5 and PEG were chose as the precursors. We found that a typical nanowire bundle is of the diameter of about 100 nm and length up to 100 μm . It is interesting to note that the cross-section of these as-prepared $\text{VO}_x \cdot \text{H}_2\text{O}$ nanowires is rectangle, obviously different from the common nanowires.

SVO nanowires

Silver vanadium oxides have been found ideally suitable for battery applications owing to their excellent electrochemical properties resulting from the variety of oxidation state of silver and vanadium. β - AgVO_3 is a stable phase and typical silver vanadium oxide. Its electrochemical property highly depends on

the composition, size, shape, crystal structure and surface properties of the product. Recently, our group synthesized AgVO_3 nanowires and AgVO_3 -PPy nanocables by rheological self-assembling process followed by in situ polymerization method.^[12] The obtained β - AgVO_3 nanomaterials have a ribbon-like morphology with the diameter of 30-500 nm and lengths ranging from several to several ten micrometers, as shown in Fig.5a. AgVO_3 -PPy nanocables can keep one dimensional structure well, but the surface of the rods has become rough.

It is found that the 1D AgVO_3 -PPy hybrid nanomaterials exhibit higher discharge capacity, capacity retention and better cycling stability compared with the pristine β - AgVO_3 nanoribbon materials (Fig.5b), resulting from the improvement of electrical conductivity due to hybrid polymerization of pyrrole accompanied by change of band structure and carrier density. Furthermore, PPy can accommodate lithium ions. When the β - AgVO_3 1D nanomaterials are enwrapped and interconnected with PPy coatings, the coated PPy layer could provide a fine pathway for electron transfer in the Li^+ ions insertion/extraction process. Thus, PPy facilitates the interfacial charge transfer and improves the utilization of the composite electrode, finally improving the electrochemical performances of the nanocables.

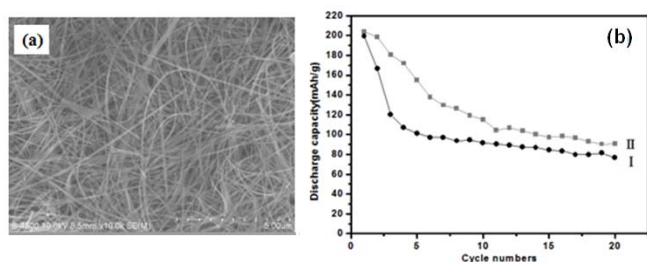


Fig.5: (a) Typical FE-SEM image of the β - AgVO_3 nanowires, (b) cyclability of the batteries assembled with the β - AgVO_3 nanowires (I) and the AgVO_3 -PPy nanocables(II).^[12]

Conclusion

Nanostructured vanadium oxides have high capacities of about 300- 650 mAh/g, which are considered as the most promising cathode materials for lithium battery. However, they will suffer from fast capacity fading during high-rate discharge/charge. The challenge is to improve the cycling stability of vanadium oxides at a high rate. Our group have used some methods such as pre-lithiation, LB assembly, Mo-doping, etc. to improve the cycling stability of nanostructured vanadium oxides.

ACKNOWLEDGEMENT

This work was supported by the National Nature Science Foundation of China (50702039), the Research Fund for the Doctoral Program of Higher Education (20070497012), and Scientific Research

Foundation for Returned Scholars, Ministry of Education of China (2008-890).

References

1. Doble, A., Ngala, K., Yang, S., Zavalij, P. Y., and Whittingham, M. S. Manganese vanadium oxide nanotubes: Synthesis, characterization, and electrochemistry. *Chem. Mater.* **13**(2001)4382–4386.
2. Krumeich, F., Muhr, H. J., Niederberger, M., Bieri, F., Schnyder, B., and Nesper, R. Morphology and topochemical reactions of novel vanadium oxide nanotubes. *J. Am. Chem. Soc.* **21**(1999)8324–8331.
3. Mai, L. Q., Chen, W., Xu, Q., Peng, J. F., and Zhu, Q. Y. Mo doped vanadium oxide nanotubes: microstructure and electrochemistry. *Chem. Phys. Lett.* **382**(2003)307-312.
4. Chen, W., Mai, L.Q., Qi, Y. Y., and Dai, Y. One-dimensional nanomaterials of vanadium and molybdenum oxides. *J. Phys. Chem. Solids*, **67**(2006)896-902.
5. Mai, L.Q., Gu, Y., Han, C. H., Hu, B., Chen, W., Zhang, P. C., Xu, L., Guo, W. L., and Dai, Y. Orientated Langmuir-Blodgett Assembly of VO_2 Nanowires. *Nano. Lett.*, **9**(2009)826-830.
6. Chen, W., Xu, Q., Hu, Y., Mai, L., and Zhu, Q. Effect of modification by poly(ethylene oxide) on the reversibility of insertion/extraction of Li^+ ion in V_2O_5 xerogel films. *J. Mater. Chem.* **12**(2002)1926-1929.
7. Chernova, N.A., Roppolo, M., Dillonb, A.C., and Whittingham, M.S. Layered vanadium and molybdenum oxides: batteries and electrochromics *J. Mater. Chem.* **10**(2009)2526-2552.
8. Ban, C., Chernova, N.A., and Whittingham, M.S. Electrospun nano-vanadium pentoxide cathode. *Electrochem. Commun.* **11**(2009)522–525.
9. Chou, S.L., Wang, J.Z., Sun, J.Z., Wexler, D., Forsyth, M., Liu, H.K., MacFarlane, D.R., and Dou, S.X. High capacity, safety, and enhanced cyclability of lithium metal battery using a V_2O_5 nanomaterial cathode and room temperature ionic liquid electrolyte. *Chem. Mater.* **20**(2008)7044–7051.
10. Chan, C.K., Peng, H., Twisten, R.D., Jarausch, K., Zhang, X.F., and Cui, Y. Fast, completely reversible Li insertion in vanadium pentoxide nanoribbons. *Nano Lett.* **7**(2007), 490-495.
11. Qiao, H., Zhu, X., Zheng, Z., Liu, L., and Zhang, L. Synthesis of $\text{V}_3\text{O}_7 \cdot \text{H}_2\text{O}$ nanobelts as cathode materials for lithium-ion batteries. *Electrochem. Commun.* **8**(2006)21-26.
12. Gao, Q., Mai, L. Q., Xu, L., Gu, Y. H., and Hu, B. Construction and electrical transport properties of one-dimensional vanadium oxide nanomaterials. *Sciencepaper Online* **5**(2010)79-87.